ARID ZONE JOURNAL OF ENGINEERING, TECHNOLOGY & ENVIRONMENT
AZOJETE June 2026. Vol.22(2):328-339
Published by the Faculty of Engineering, University of Maiduguri, Maiduguri, Nigeria.
Print ISSN: 1596-2490, Electronic ISSN: 2545-5818
https://doi.org/10.63958/AZOJETE/2026/22/02/011
www.azojete.com.ng

ORIGINAL RESEARCH ARTICLE

EXPERIMENTAL INVESTIGATION AND PREDICTIVE MODELLING OF SUSTAINABLE CONCRETE INCORPORATING RICE HUSK ASH AND PERIWINKLE SHELL ASH

T. A. Ibu*, A. Aboshio, A. Alhassan

Department of Civil Engineering, Bayero University, Kano
Corresponding author's email: tomibu18@gmail.com

ARTICLE INFORMATION

Received: 27th February 2026
Revised: 29th April 2026
Accepted: 30th April 2026

Keywords:
Compressive strength
Modeling
Optimization
Periwinkle shell ash (PSA)
Rice Husk Ash (RHA)
Splitting tensile strength
Supplementary cementitious materials (SCM)
Sustainability

ABSTRACT

Concrete remains the most widely used construction material globally but the durability and performance of concrete structures have become a critical concern in modern construction. Concrete is exposed to chemical attacks that significantly affect its long-term strength and integrity. This study investigated the properties of concrete incorporating blended Rice Husk Ash (RHA) and Periwinkle Shell Ash (PSA) as supplementary cementitious materials, and also developed predictive strength models. Concrete mixes with varying RHA-PSA replacement ratios were produced at a constant water–cement ratio of 0.55 and cured for 3, 7, 28, and 90 days. The ashes were characterized using Energy-Dispersive X-Ray Fluorescence (EDXRF). While aggregates conforming to BS EN standards were used, workability test were performed on the fresh concrete samples and compressive strength, tensile strength, and density were done on the hardened samples. Finally, the properties were modelled and validated using regression analysis. The results indicated that both RHA and PSA contained key oxides (CaO, SiO_2, Al_2O_3, Fe_2O_3). Also, RHA satisfied the ASTM C618 requirement of the sum of SiO_2, Al_2O_3 and Fe_2O_3 of more than 70% with a value of 71.86% indicating their pozzolanic potential. PSA, with a combined total of 3.17% did not meet this pozzolanic threshold but complemented RHA with its high CaO (≈ 88%). RHA and PSA had specific gravities of 1.79 and 2.49 respectively, indicating their potential as lightweight pozzolans, reducing concrete density while maintaining strength. At 28 days, 70% of mixes exceeded the 25 N/mm² target strength, with B7(6%RHA + 4% PSA) achieving the highest compressive strength and B6(5.25%RHA + 4.75% PSA) the highest tensile strength at 28 - 90 days. Predictive models of (R^2 = 0.8410) for compressive strength, and (R^2 = 0.5899) for splitting tensile strength at 28days curing respectively accurately described strength development for specific mix designs. B7 mix design was recommended where high compressive strength was a priority. While B6 mix ratio is preferable for maximizing splitting tensile strength for cubes/cylinders cured in water. Balanced blend of ≈5–6% RHA and 4–5% PSA enhanced strength, durability, and microstructure, promoting sustainable, high-performance concrete.

1.0 Introduction

The global push for sustainable construction has increased interest in using agricultural and marine by-products as supplementary cementitious materials (SCMs). Cement production contributes substantially to CO_2 emissions, while agricultural and marine wastes accumulate, particularly in Nigeria. Rice Husk Ash (RHA), a highly pozzolanic by-product of rice husk combustion, contains 64% amorphous silica, promoting secondary C–S–H formation and improving concrete durability (Aboshio *et al.*, 2023; Labador *et al.*, 2024; Mehri and Taghavi, 2023). Periwinkle Shell Ash (PSA), derived from calcined shells, is lime-rich (≈88% CaO)

and accelerates early hydration (Inyang and Etuk, 2016; Offiong and Akpan, 2017). Despite individual studies on RHA and PSA, both substances have not effectively shown their pozzolanic impacts. Limitations on their usage still exist and their combined effect remains unexplored. Thus, there is a need to investigate into their synergistic effect on mechanical properties and predictive strength modelling. Theoretically, their combination may produce synergetic effects, with RHA's high silica content promoting (C-S-H) formation and PSA's calcium-rich composition contributing to calcium aluminate hydrate (C-A-H) gels. Together these compounds can densify the concrete matrix, fill pores, lower permeability, and significantly improve durability (Umasabor and Osinubi, 2012). Their beneficial incorporation into concrete production presents a multifaceted opportunity: reducing OPC demand (associated CO^2 emission), lowering construction costs, enhancing the durability of structures, and promoting sustainable waste management.

The replacement of Rice Husk Ash (RHA) and Periwinkle Shell Ash (PSA) adopted in this study were selected based on a combination of literature evidence and statistical design requirements. Previous studies have established that optimum performance level of RHA typically lies within the range of 5-15% (Nishant and Vinod, 2015), while PSA has been reported to exhibit optimal performance at approximately 10% replacement (Dahunsi and Bamisaye, 2002; Umoh and Olusola, 2012), beyond which strength reduction may occur due to dilution effect and increased porosity. Consequently, the experimental domain for both materials were restricted to a maximum of 10% replacement, ensuring the study remained within the feasible performance-level region.

Accordingly, 0% replacement was included to serve as the control mix. 10% replacement was adopted as the upper bound, representing the practical optimum limit reported in literature (Nishant and Vinod, 2015: Dahunsi and Bamisaye, 2002; Umoh and Olusola, 2012). To enhance the accuracy of optimization of the most promising region, intermediate replacement levels were concentrated within 5-6% for RHA, and 4-5% for PSA, where previous studies suggested high sensitivity of mechanical performance. These intermediate values were not arbitrary selected but were generated using Design-Expert software as part of response surface design to enable precise modelling of curvature and interaction effects.

2. Materials and Method

2.1 Materials

2.1.1 Cement

Ordinary Portland Cement (OPC) was procured from a local dealer in Rijiyar Zaki, Kano.

2.1.2 Aggregates

River sand from the Challawa River was used as fine aggregate, and 20 mm crushed granite (coarse) obtained from Rimi Gado quarry, Kano, per (BS EN 933-1:2012).

2.1.3 Rice Husk Ash (RHA)

Rice husks purchased from local dealers in Konor Dawaki, Kano and calcined at 700°C for 2 h; sieved to 150 µm. The particle size (150 µm) was necessary as to balance reactivity and workability with that of PSA sieved to a lower microbe (75 µm), as finer particles alone may increase water demand (Akinwumi and Aidom, 2015: Olutoge and Amusan, 2014).

2.1.4 Periwinkle Shell Ash (PSA)

Periwinkle shells sourced from Calabar beach markets in Calabar Town, Cross River state was washed, dried, and calcined at 900°C for 1 h then sieved to 75 µm.

2.1.5 Water

Potable laboratory water obtained from the Civil Engineering Laboratory, Bayero University, Kano met ASTM C1602/C1602M-18 specification.

2.2 Methods

Corresponding author's email address: tomibu18@gmail.com

2.2.1 Particle size distribution

Samples (1000g each) of aggregates were mechanically agitated for five minutes, and the retained mass on each sieve was recorded to compute cumulative passing percentages in accordance with (BS EN 933-1:2012)

2.2.2 Specific gravity

The specific gravity of RHA, PSA, Fine, and Coarse aggregates was determined in accordance with ASTM C128-2022 for fine aggregates and ASTM C127-2015 for coarse aggregates.

2.2.3 Chemical composition

Oxide compositions of RHA and PSA were determined using Energy-Dispersive X-Ray Fluorescence (EDXRF) at Umaru Musa Yar'adua University, Katsina.

2.2.4 Concrete mixes

Ten mixes featuring varying RHA–PSA ratios were casted at a constant water- to-cement ratio of 0.55, with a combined optimal replacement content of 10% (Tables 1 & 2).

Table 1: Percentage replacement of cement with RHA and PSA (adapted from design expert, 2023)

Concrete Material	B1	B2	B3	B4	B5	B6	B7	B8	B9	B10
RHA (%)	0	6	10	0	0	5.25	6	5.5	5.75	5
PSA (%)	0	0	0	6	10	4.75	4	4.5	4.25	5

Table 2: Concrete mix quantities

Materials	**Cement**	**Fine Agg.**	**Coarse Agg.**	**Water**
Quantity per cubic(kg) /m^3	**346**	**663**	**1232**	**190**

2.2.5 Workability

The Slump test was conducted on fresh concrete in accordance with BS EN 12350- 2:2000.

2.2.6 Compressive strength test

Concrete cubes (100 × 100 × 100 mm) were cured in water and tested at 3, 7, 28, 90 days using a digital compression machine of 2000 kN capacity in accordance with BS EN 12390-3: 2009

2.2.7 Splitting tensile strength

Concrete cylinders (100 × 200 mm) were tested at the same ages and curing medium in accordance with BS EN 12390-6:2009.

2.2.8 Density

Density was determined after 24 h ambient temperature post-curing in water in accordance with BS 1881-114:1983.

2.2.9 Curing medium

Concrete samples were cured in water for 3, 7, 28, 90 days respectively.

Corresponding author's email address: tomibu18@gmail.com

2.2.10 Predictive modelling

Regression analysis for compressive and tensile strength was performed using MATLAB Version R2023a - 2023 (Mathworks, 2023).

3. Results and Discussion

3.1 Chemical Composition of RHA and PSA

Table 3 gives elemental composition of RHA and PSA using Energy-Dispersive X-Ray Fluorescence (EDXF), and comparing with that of OPC. PSA contains CaO ≈ 88%, SiO_2 ≈ 1.4% (high-lime pozzolan). RHA: SiO_2 ≈ 64%, CaO ≈ 1.2% (silica-rich, highly reactive). Blending RHA and PSA mimics OPC balance, optimizing pozzolanic reactions. Blending RHA with PSA and OPC was to create a more chemically balanced binder, where PSA supplies CaO for hydration and RHA provided silica for pozzolanic reactions, potentially enhancing strength, durability, and resistance to any chemical aggression. This synergy was the central justification for their combined use (Hossain and Islam, 2022).

Table 3: Oxide Composition of OPC, RHA, and PSA

Oxide	OPC (%)	RHA (%)	PSA (%)
CaO	63.0	1.2	88.0
SiO_2	20.0	64.0	1.4
Al_2O_3	6.0	7.3	0.79
Fe_2O_3	3.0	0.56	0.49
TOTAL	**92**	**73.06**	**90.68**

3.2 Fresh and Hardened Properties of Concrete

3.2.1 Properties of aggregates

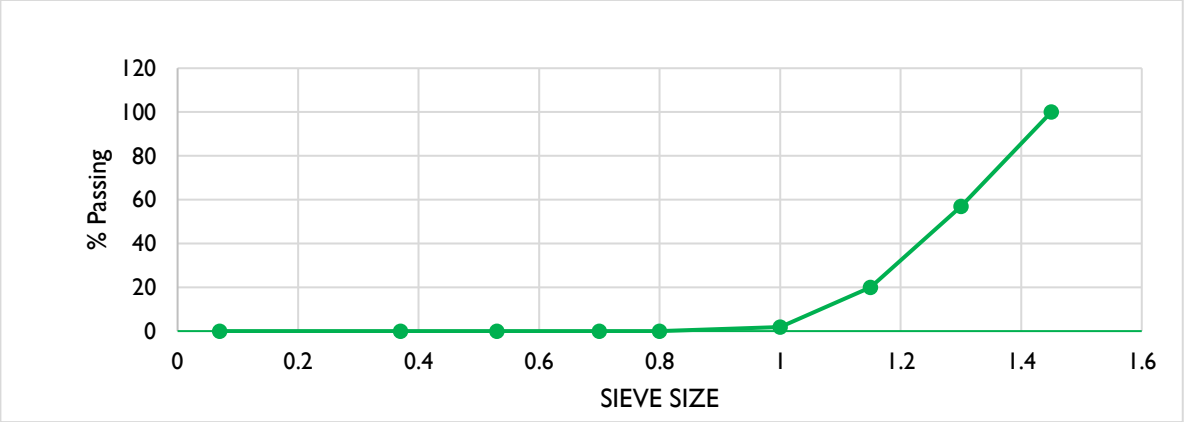

Figure 1a: Particle size distribution of coarse aggregates

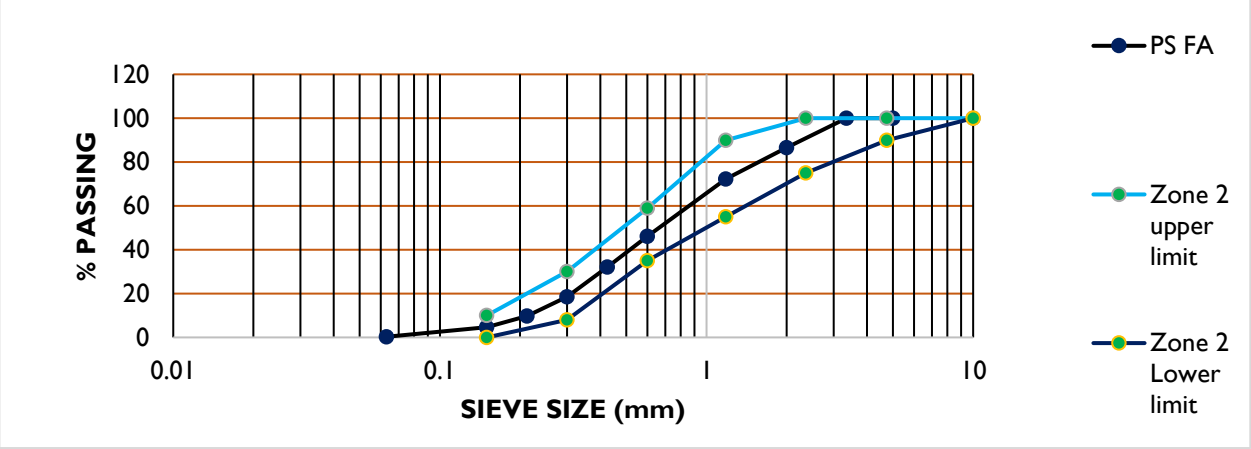

Figure 1b: Particle size distribution of fine aggregates

Corresponding author's email address: tomibu18@gmail.com

Figures 1a, and 1b present the gradation of aggregates. Coarse aggregates confirm a nominal size of 20 mm, consistent with (BS EN 206-2013) for structural concrete. Aggregate sizes above 20 mm reduce flowability and passing ability, leading to poor compaction. The Fine aggregates falls within class 2 (BS 882--1992), in the range 63 µm to 2 mm, with the 600 µm sieve retaining the largest fraction (≈26%). This grading ensures adequate packing and workability, aligning with BS EN 206 (2013) recommendations for fine aggregates in structural concrete.

The aggregate property satisfies international standard, ensuring that observed performance variations can be attributed primarily to the RHA-PSA admixtures rather than inconsistencies in aggregate grading.

3.2.2 Specific gravity of aggregates

Table 4 presents the specific gravity values of the investigated materials. PSA recorded 2.49, RHA 1.79, fine aggregate 2.58, and coarse aggregate 2.71. These values fall within the acceptable ranges for normal-weight aggregates (ASTM C127/128-15/22). The relatively low specific gravity of RHA reflects its highly porous microstructure and the influence of calcination temperature.

PSA exhibited a higher specific gravity 2.49. Its density is closer to that of natural aggregates (typically around 2.5 - 2.7) and OPC (around 3.1 - 3.2), confirming its suitability as a partial replacement without significantly compromising the unit weight of concrete. The combined use of RHA (lightweight, silica-rich) and PSA (denser, lime-rich) thus offers complementary advantages: reduced density for sustainability, balanced by adequate weight and strength development.

Table 4: Specific gravity of materials

Material	RHA	PSA	Fine Aggregate	Coarse Aggregate
Specific Gravity	1.79	2.49	2.58	2.71

3.2.3. Workability test result

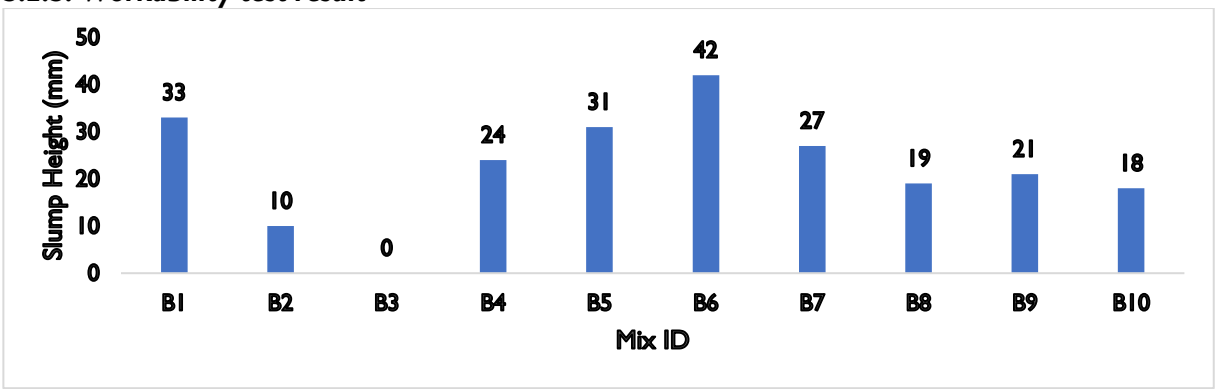

Figure 2: Slump test of concrete mixes

Figure 2 illustrates slump test results for concrete mixes with varying RHA and PSA percentages. Mix B6(5.25%RHA + 4.75% PSA) achieved a slump of 42mm, the control mix B1(0%RHA + 0% PSA) recorded a slump of 33mm, while B5(10% PSA) recorded 31mm, all within the design range of 30-60mm, indicating good workability. Mix B3 (10% RHA) had zero slump, indicating a harsh, unworkable mix due to high water demand from RHA's high surface area and porosity. (Zhang *et al.,* 2022*;* Kamau *et al.,* 2017)

3.2.4. Compressive Strength

Figure 3 presents the compressive strength evolution of RHA-PSA concretes (B1-B10) cured for 3-90 days. The compressive strength results show the characteristic-age relationship, with all mixes exhibiting progressive strength gain from 0 to 90 days. The most rapid increase occurred between 7 and 28 days, followed by a slower gain up to 90 days. The highest strengths at 28-90 days (~32-35 N/mm²) were recorded by mixes such as B1, B6, B7 and B9, while the lowest, such as B3, plateaued below ~20 N/mm². This trend reflects the combined effects of cement hydration and pozzolanic reactions-rapid early-age hydration from calcium-rich components and sustained late-age gains from siliceous materials (Neville, 2011; Mehta & Monteiro, 2014).

Corresponding author's email address: tomibu18@gmail.com

At early ages (≤7 days), mixes with higher initial strength, such as B5, are likely PSA-dominant or contain higher CaO contents. PSA in this study contains approximately 88% CaO, which accelerates hydration by forming abundant portlandite ($Ca(OH)_2$), thus boosting early-age strength (Offiong and Akpan, 2017; Inyang & Etuk, 2016; Nwankwo, and Ezeokonkwo 2022). In contrast, mixes with slower early strength gain, such as B3 (10%RHA), were consistent with RHA-rich compositions. RHA, with its high amorphous silica content (>60%), reacts slowly in the early curing period, resulting in lower early strength but progressive improvement at later ages (Holland, 2005, 2005; Ganesan *et al.,* 2008; Ahmad *et al.,* 2020).

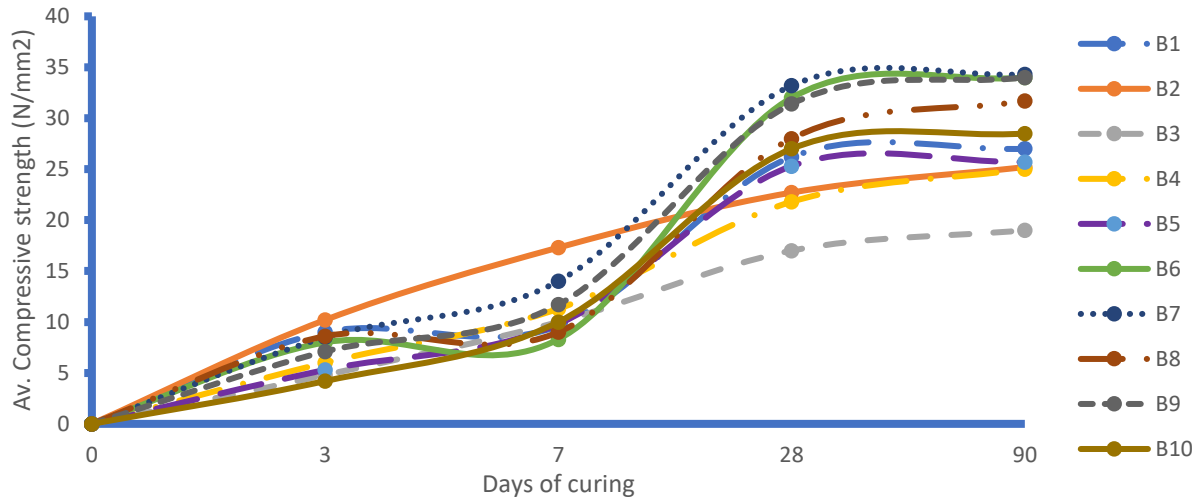

Figure 3: Compressive strength vs. curing age

Between 28 and 90 days, the highest performing blends (B6, B7, and B9) suggested a balanced combination of RHA and PSA. PSA provided the initial Ca (OH) $_2$, which RHA subsequently consumed through pozzolanic reactions to form additional calcium silicate hydrate (C-S-H). This process refined pore structure, reduced permeability, and sustained strength gains beyond the conventional 28-day mark (Zhang and Malhotra, 1996; Khan *et al.,* 2020; Singh *et al.,* 2020). Conversely, PSA-rich blends peaked early but exhibited limited long-term improvement once free portlandite was depleted, while RHA-rich blends improved gradually.

3.2.5 Splitting tensile test

Figure 4 presents the splitting tensile strength of RHA-PSA blended concretes (B1-B10). The splitting tensile strength results indicated a progressive increase in strength with curing age for all specimens (B1-B10), reflecting the continuous hydration of cementitious phases and the pozzolanic contribution of rice husk ash (RHA) and periwinkle shell ash (PSA) blends.

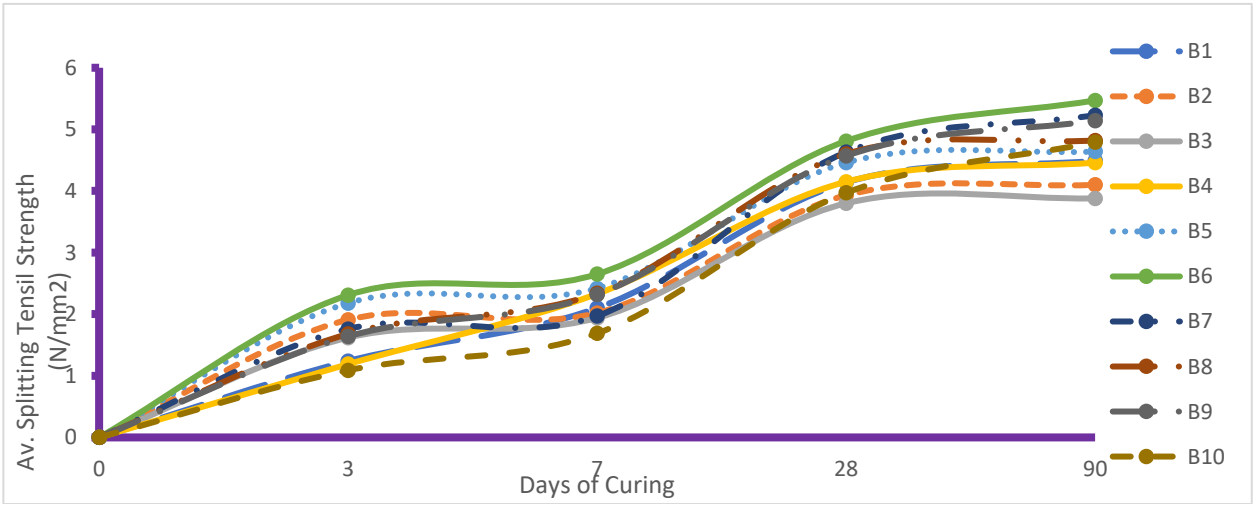

Figure 4: Splitting tensile strength vs. curing age

At early ages (3-7 days), strength development was relatively modest across all specimens, which aligns with the findings of Neville (2011) that tensile strength gain in concrete is slower than compressive strength due to the lower contribution of hydration products to tensile resistance in the early stages. The blends

containing higher pozzolanic content, particularly B6, showed slightly better early tensile strength, suggesting a beneficial filler effect that enhanced packing density and early bond formation (Chindaprasirt *et al.,* 2007).

From 7 to 28 days, there was a more pronounced increase in splitting tensile strength, with B6 attaining the highest value. This period coincided with the pozzolanic reaction becoming more dominant, consuming calcium hydroxide and forming additional C-S-H gel, which refined the microstructure and improved tensile resistance (ASTM C618-023; Thomas, 2007). Specimens such as B3 and B4 recorded slightly lower gains, which may be attributed to higher replacement levels that reduced the available clinker content, slowing early hydration.

By 90 days, most specimens plateaued, with B6, B7, and B9 maintaining superior strengths above 5N/mm², consistent with Mehta and Monteiro (2014) who reported that supplementary cementitious materials enhanced long-term tensile performance due to continued pozzolanic activity. The slightly lower final strength in B3 and B4 further supports the balance required between cement and pozzolan to achieve optimal tensile capacity.

3.2.5 Density Test Result

Figures 5 and 6 present the density results for concrete cubes and cylinders. The result for density of cubes showed a progressive increase with age up to 90 days, with B7 presenting the highest and B2 lowest density at 90 days of curing. B7, B6, B5 had a higher density when compared with the control. The result for density of cylinders also showed a progressive increase with age up to 90 curing days, with B8 presenting the highest at 90 days of curing. Both results presented showed a synergistic effect of Rice Husk Ash and Periwinkle Shell forming denser microstructure, filling of pores, improvement of cement hydration, thus reducing overall porosity and enhancing the density of the concrete (ACI Committee 232, 2014).

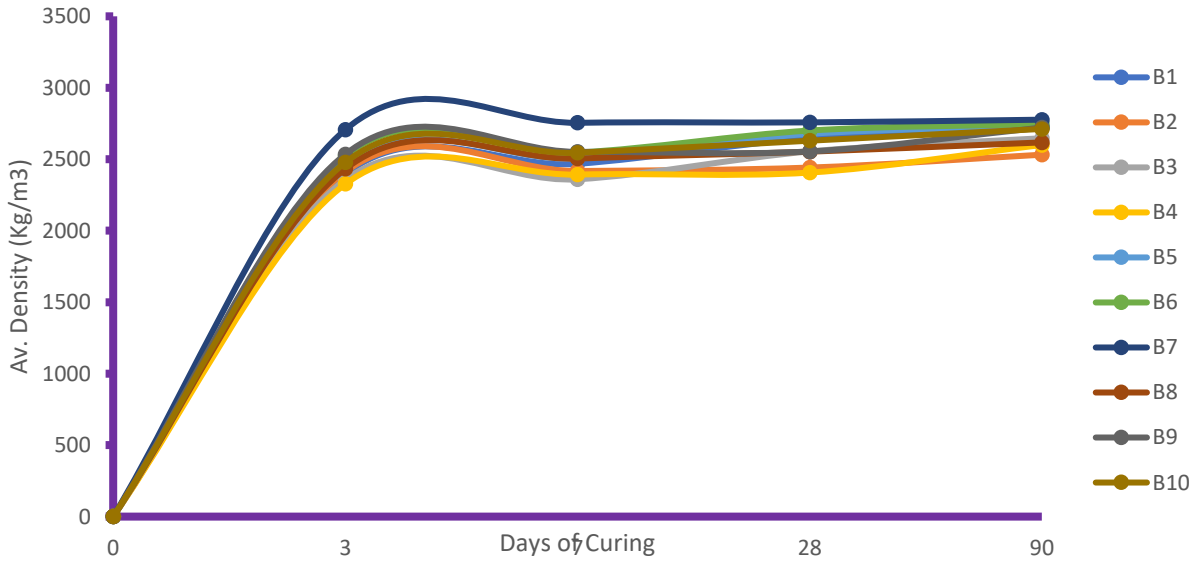

Figure 5: Cube density vs. curing age

3.2.7. Predictive Modeling

i. Compressive Strength Models

The following models (Eqns. 1 & 2) were obtained based on 28-day and 90-day curing days as the best-fit:

At 28 Days Curing:

$$CS = 26.20 - 0.15810X - 1.6537Y - 0.0729X^2 + 0.4639XY + 0.1534Y^2 \quad (1)$$

At 90 Days Curing:

$$CS = 27.00 + 3.9279X - 0.9690Y - 0.4685X^2 + 0.0330XY + 0.0810Y^2 \quad (2)$$

Corresponding author's email address: tomibu18@gmail.com

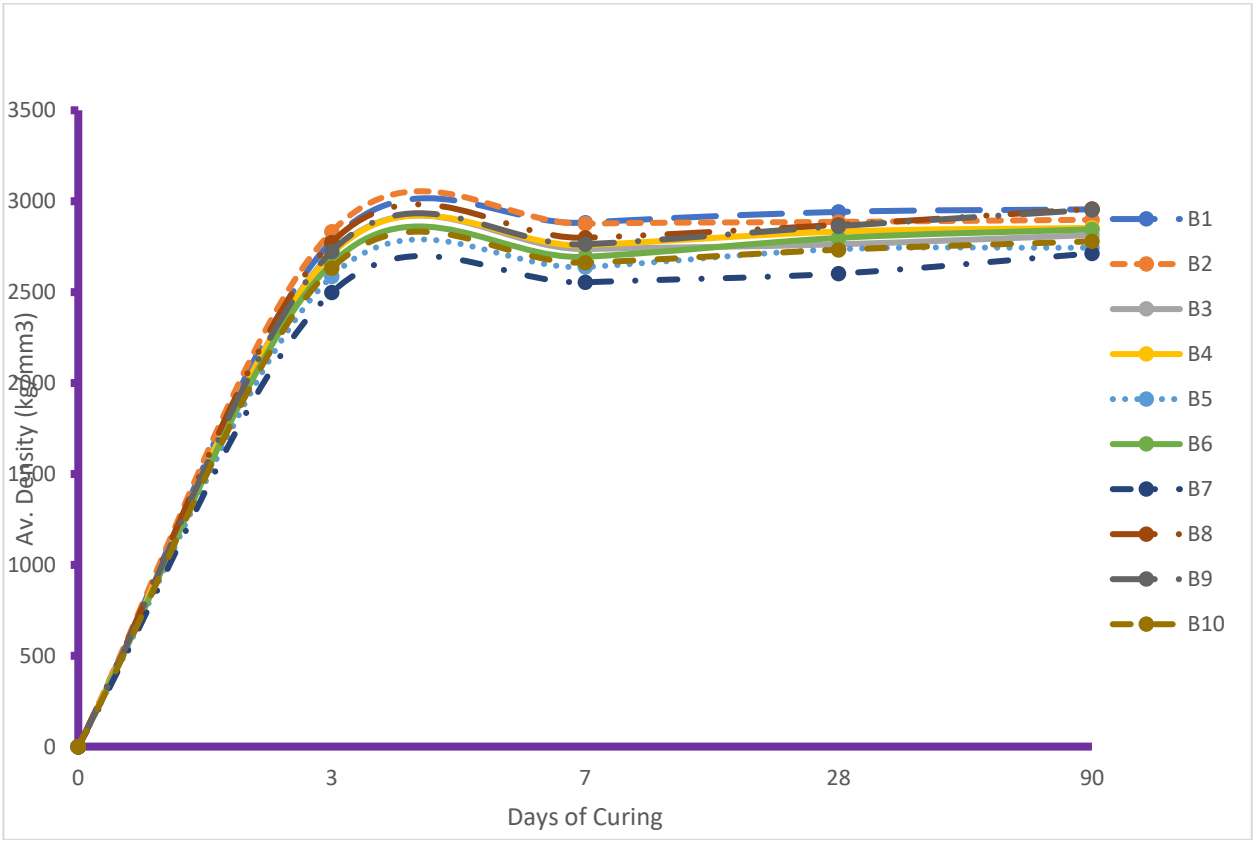

Figure 6: Cylinder density vs. curing age

Table 5 presents the statistical performance of second-order regression models developed to predict the compressive strength of concrete containing Rice Husk Ash (RHA) and Periwinkle Shell Ash (PSA) at 28 and 90 days of curing. Evaluation metrics such as the sum of squared errors (SSE), R-squared (R^2), adjusted R^2, and root mean square error (RMSE) confirm model accuracy and reliability.

At 28 days of curing, the adjusted R^2 (0.6422) accounts for the polynomial structure of the model, while the RMSE of 3.0236 N/mm² fitted well within the 2-5 N/mm² range suggested by Zain and Abd (2009), affirming the model's use for early-age strength prediction. By 90 days curing, the adjusted R^2 of 0.7175 further supported model efficiency. A lower RMSE of 2.7856 N/mm² confirmed better predictive precision at later ages, consistent with the enhanced pozzolanic activity of RHA noted by Ganesan *et al.* (2008).

Table 5: Goodness-of-Fit Statistics for Compressive Strength Model

Metric	**28 Days**	**90 Days**
R-Squared (R^2)	0.8410	0.8745
Adjusted R^2	0.6422	0.7175

ii *Splitting tensile strength models*

The following models (Eqns. 3 & 4) were obtained based on 28-day and 90-day curing days as the best-fit:

At 28 Days Curing:

$$\text{STS} = 4.14 - 0.04200X - 0.0397Y - 0.0012X^2 + 0.0247XY + 0.0069Y^2 \quad (3)$$

At 90 Days Curing:

$$\text{STS} = 4.49 - 0.0747X - 0.0325Y - 0.0016X^2 + 0.0411XY + 0.0046Y^2 \quad (4)$$

Table 6 presents the performance of second-order regression models developed to predict the splitting tensile strength (STS) of concrete incorporating Rice Husk Ash (RHA) and Periwinkle Shell Ash (PSA) at 28 and 90 days. The models were assessed using SSE, R^2, adjusted R^2, and RMSE to evaluate accuracy and predictive capability.

Corresponding author's email address: tomibu18@gmail.com

At 28 days curing, the model produced an SSE of 0.4516 and an R^2 of 0.5899, indicating that about 59% of the variance in tensile strength is explained by RHA and PSA content. Also, the relatively lower predictive performance obtained (R^2 = 0.5899) was likely because this response variable was more challenging to model accurately than other mechanical properties. This may be attributed to the inherently complex failure mechanism of splitting tensile strength, which is highly sensitive to microcracks, internal voids, aggregate-paste interfacial bonding, specimen preparation, curing conditions, and minor testing inconsistencies. Unlike compressive strength, tensile failure is often governed by localized weaknesses and microstructural heterogeneity that may not be fully represented by the selected input parameters (Neville, 2011). Additionally, the variability may also reflect limitations in dataset size and the presence of nonlinear relationships among the governing factors. Therefore, while the model showed moderate predictive capacity, further improvement may be achieved by incorporating additional descriptors related to microstructure, curing regime, and material consistency, as well as by optimizing model hyperparameters.

The adjusted R^2 of 0.0772 suggested that not all polynomial terms contribute significantly at this early stage, likely due to the delayed pozzolanic reaction of RHA. Nonetheless, the RMSE of 0.3364 N/mm^2 demonstrated acceptable prediction accuracy, aligning with performance thresholds reported by Zain and Abd (2009) and Charhate *et al.* (2018).

By 90 days of curing, model accuracy improves substantially. The SSE drops to 0.3659, and the R^2 rose to 0.8357, showing excellent alignment between predicted and experimental values. The adjusted R^2 of 0.6304 confirmed the relevance of the model's non-linear structure, while the RMSE of 0.3025 N/mm^2 further affirmed its high predictive accuracy.

Table 6: Model Performance for Splitting Tensile Strength

Metric	28 Days	90 Days
R-Squared (R^2)	0.5899	0.8357
Adjusted R^2	0.0772	0.6304

iii. Application

The developed models predicted the properties of concrete incorporating blended Rice Husk Ash (RHA) and Periwinkle Shell Ash (PSA) as supplementary cementitious materials. Concrete mixes with varying RHA–PSA replacement ratios were produced at a constant water–cement ratio of 0.55 and cured for 3, 7, 28, and 90 days. The models can be used for predicting compressive and splitting tensile strength of the mixes at curing ages of 28 and 90 days. The models are therefore, recommended for practical use due to their higher accuracy and ability to represent the observed trends.

4. Conclusion

1. The study revealed that both Rice Husk Ash (RHA) and Periwinkle Shell Ash (PSA) contain the primary oxides found in cement, namely Calcium Oxide (CaO), Silicon Dioxide (SiO_2), Aluminum Oxide (Al_2O_3), and Iron (III) Oxide (Fe_2O_3) in varying proportions.

2. The chemical compositions of PSA and RHA highlight their complementary roles in concrete production. PSA's high CaO content (88%) supports the formation of Ca $(OH)_2$, which, when combined with RHA's high SiO_2 content (64%), triggers a pozzolanic reaction forming C-S-H.

3. The specific gravity of PSA (2.49) and RHA (1.79) indicates their potential as lightweight pozzolans, reducing concrete density while maintaining strength.

5. 70% of all the compressive strength mixes surpassed the 25 N/mm^2 design strength at 28 days, with continued strength gain to 90 days. B7(6%RHA + 4%PSA) recorded the highest strength. Whereas, B6(5.25%RHA + 4.75%PSA) achieved the highest values at both 28 and 90 days for the Splitting tensile strength.

7. Density improved with age; B7(6%RHA + 4%PSA) had the highest cube density and B8 the highest cylinder density at 90 days.

Corresponding author's email address: tomibu18@gmail.com

8. The optimal blends in this study (≈5-6% RHA and 4-5% PSA) provide both adequate early performance and superior long-term strength. This offers sustainable, high performance alternatives to OPC and its associated hazards.

9. The predictive capability, R^2 = 0.8410 at 28 days curing and R^2 = 0.8745 at 90 days curing gave the best fit equations for predicting compressive strength. While, (R^2 = 0.5899) and (R^2 = 0.8357) at 28 days and 90 days respectively for splitting tensile strength prediction equations. Other evaluation metrics such as the sum of squared errors (SSE), R-squared (R^2), and root mean square error (RMSE) confirm model accuracy and reliability.

Based on the findings of this study, the following recommendations are made:

1. The B7 mix ratio is recommended where high compressive strength is a priority, while the B6 mix ratio is preferable for maximizing splitting tensile strength for cylinders cured in water.
2. RHA and PSA should be considered as supplementary cementitious materials in sustainable construction, particularly in regions with abundant agricultural and marine waste.
3. The developed strength prediction models can be applied for preliminary mix design and quality control in concrete production involving RHA–PSA blends at 28- and 90-day curing.
4. To further enhance prediction of splitting tensile strength, future work may consider feature expansion, hyperparameter tuning, outlier analysis, and the inclusion of additional variables that directly characterize tensile failure behavior.

References

Aboshio, A. Shuaibu, HG. and Abdulwahab, MT. 2023. Properties of Rice Husk Ash Concrete with Periwinkle Shell as Coarse Aggregates. *Nigeria Journal of Technological Development*.

ACI Committee 232, 2014: ACI 232.2R-14: Report on the Use of Rice Husk Ash in Concrete

Ahmad, J., Tufail, RF. and Aslam, M. 2020. Effect of Rice Husk Ash on the Mechanical Properties of Concrete. Journal of Building Engineering, 32: 101758. doi: 10.1016/i.jobe.2020.101758

Akinwumi, II. and Aidom, OO. 2015. Effect of Rice Husk Ash on Workability and Strength Properties of Concrete. Journal of Civil Engineering and Architecture, 9(6): 669-677.

ASTM C127/128-15/22. Standard Specification for Determining the Relative Density and Absorption of Fine and Coarse Aggregates. West Conshohocken, PA, U.S.A. ASTM International,

ASTM C1602/C1602M-18. Standard Specification for Mixing Water Used in the Production of Hydraulic Cement Concrete. West Conshohocken, PA, U.S.A. ASTM International,

ASTM International, ASTM C618 -2023. Standard Specification for Coal Fly Ash and Raw or Calcined Natural Pozzolan for Use in Concrete, ASTM International, West Conshohocken, PA, USA. DOI:10.1520/c0618-23A

BS 1881, Part 114:1983 – Testing Concrete Methods for Determination of density of hardened concrete, Her Majesty Stationary Office, 2 Park Street London CIABS

BS 882 -1992. Testing Aggregates. Methods of Determination of Particle Size.

BS EN 12350, Part 2 -2000. Testing Concrete. Methods for determining Slump.

BS EN 12390, Part 3: 2009. Testing Hardened Concrete: Compressive Strength of Test Specimens. London, U.K. British Standards Institute.

BS EN 12390, Part 6: 2009. Testing Hardened Concrete: Tensile Splitting Strength of Test Specimens. London, U.K. British Standards Institute.

BS EN 206:2013. Additional Rule for Self-Compacting Concrete. British Standards Publication.

Corresponding author's email address: tomibu18@gmail.com

BS EN 933, Part 1. -2012. Test for Geometrical Properties of Aggregates. Determination of the Particle Size Distribution, Sieving Method.

Charhate, S., Subhedar, M. and Adsul, N. 2018. Prediction of Concrete Properties Using Multiple Linear Regression and Artificial Neural Network. J. Soft Comput. Civ. Eng. 2. https://doi.org/10.22115/scce.2018.112140.1041

Chindaprasirt, P., Homwuttiwong, S., and Sirivivatnanon, V. 2007. Influence of fly ash fineness on strength, drying shrinkage and sulfate resistance of blended cement mortar. *Cement and Concrete Research*, 37(1), 108–115.

Ganesan, K., Rajagopal, K. and Thangavel, K. 2008. *Rice husk ash blended cement: Assessment of optimal level of replacement for strength and permeability properties of concrete*. Construction and Building Materials, 22 (8):1675–1683. doi: 10.1016/j.conbuildmat.2007.06.011

Woodhead . https://WWW.silicafume.org/pdf/silicafume-users-manual.pdf.

Holland, TC. 2005. *Silica fume user's manual*. FHWA-HRT-05-004.

Inyang, AE. and Etuk, BR. 2016. *The Effect of Calcination Temperature on the Chemical Composition of Oyster, Periwinkle and Snail Shell Ash*. International Journal of Research in Engineering and Technology. 5(08): 200-203.

Kamau, J., Ahmed, A., Hyndman, F., Hirst, P. and Kangwa, J. 2017. Influence of Rice Husk Ash Density on the Workability and Strength of Structural Concrete. European Journal of Engineering Research and Science, 2 (3): 36

Labador, CKC., Mon Bryan, ZG. And Roy, BT. 2024. Mechanical Properties of Concrete Blended with Rice Husk Ash, Oyster Shell Powder, and Ferrous Powder. *Engineering Materials*: 117–123.

Mehri, S. and Taghavi, S. 2023. Physical and Mechanical Properties Investigation of Concrete with Periwinkle Shell Ash and Recycled Aggregates. *Journal of Civil Aspects and Structural Engineering*.

Mehta, PK. and Monteiro, PJ. 2014. Concrete: Microstructure, Properties, and Materials (4th ed.). McGraw-Hill Education.

Neville, AM. 2011. *Properties of Concrete*, 5th ed. Pearson Education.

Nishant, K. and Vinod, M. 2015. Influence of Rice Husk Ash on the Properties of Concrete. Journal of Computer Science and Engineering.1 (5): 1-10

Nwankwo, CO., and Ezeokonkwo, JC. 2022. Influence of Periwinkle Shell Ash on the durability Properties of Concrete, Construction and Building Materials, 323, 126546

Offiong, UD. and Akpan, GE. *2017. Assessment of Physico-Chemical Properties of Periwinkle Shell Ash: A Partial Replacement for Cement in Concrete.* International Journal of Scientific Engineering and Science. 1(7): 33-36.

Olutoge, FA. and Amusan, GM. 2014. The Effect of Rice Husk Ash and Periwinkle Shell Ash on the Properties of Concrete. Journal of Emerging Trends in Engineering and Applied Science, 5(2): 1

Singh, M., Awal, ASMA. and Agarwal, SK. 2020. *Supplementary cementitious materials for sustainable concrete*. Material Today: Proceedings. 32: 845-852.

STAT-EASE, INC. 2023. Design-Expert (Version 13). Minneapolis, MN: STAT-EASE, INC.

The MathWork, Inc. MATLAB (Version R2023a). Natick, Massachusetts, United States.

Thomas, MDA. 2007. Optimizing the use of fly ash in concrete. *Portland cement Association*.

Corresponding author's email address: tomibu18@gmail.com

The Math Work, Inc. MATLAB (Version R2023a). Natick, Massachusetts, United States.

Umasabor, RI. and Osinubi, KJ. 2021. Synergistic Effect of Combining Rice Husk Ash and other Supplementary Cementitious Materials on the Properties of Concrete. Journal of Building Engineering, 44. 102931.

Umoh, AA and Olusola, KO. 2012. *Strength Characteristics of Periwinkle Shell Ash Blended Cement Concrete*. International Journal of Architecture, Engineering and Construction. 1(4): 213-220.

Zain, MFM. and Abd, SM. 2009. Multiple regression model for compressive strength prediction of high-performance concrete. J. Applied. Science. 9: 155–160. https://doi.org/10.3923/jas.2009.155.160

Zhang, C., liu, H., and Liu, C. 2022. Impact of Rice Husk Ash on the Mechanical Characteristics and Freeze-The Resistance of Recycled Aggregate Concrete. Applied Sciences, 12(23). doi:12.3390/app122312238

Zhang, MH., & Malhotra, VM. 1996. *High-performance concrete incorporating rice husk ash as a supplementary cementing material*. ACI Materials Journal, 93(6): 629–636.

Corresponding author's email address: tomibu18@gmail.com